Automatica 66 (2016) 262–270

Contents lists available at ScienceDirect

Automatica

journal homepage: www.elsevier.com/locate/automatica

Brief paper

Split-path nonlinear integral control for transient performance improvement☆

S.J.L.M. van Loon, B.G.B. Hunnekens, W.P.M.H. Heemels, N. van de Wouw [1], H. Nijmeijer

Eindhoven University of Technology, Department of Mechanical Engineering, P.O. Box 513, NL 5600 MB Eindhoven, The Netherlands

ARTICLE INFO

Article history:
Received 9 October 2014
Received in revised form
16 July 2015
Accepted 22 December 2015
Available online 27 January 2016

Keywords:
Transient performance
Split-path nonlinear control
Stability
Hybrid control
Motion control

ABSTRACT

In this paper, we introduce the split-path nonlinear integrator (SPANI) as a novel nonlinear filter designed to improve the *transient* performance of linear systems in terms of overshoot, while preserving good rise-time and settling behavior. In particular, this nonlinear controller targets the well-known trade-off induced by integral action, which removes steady-state errors due to constant external disturbances, but deteriorates transient performance in terms of increased overshoot. The rationale behind the proposed SPANI filter is to ensure that the integral action has, at all times, the same sign as the closed-loop error signal, which, as we will show, enables a reduction in overshoot thereby leading to an overall improved transient performance. The resulting closed-loop dynamics is modeled by a hybrid dynamical system, for which we provide sufficient Lyapunov-based conditions for stability. Furthermore, we illustrate the effectiveness, the design and the tuning of the proposed controller in a benchmark simulation study of an industrial pick-and-place machine.

1. Introduction

In classical linear control theory, it is well-known that Bode's gain–phase relationship causes a hard limitation on achievable performance trade-offs in linear time-invariant (LTI) feedback control systems, see, e.g., Freudenberg, Middleton, and Stefanpoulou (2000) and Seron, Braslavsky, and Goodwin (1997). The related interdependence between gain and phase is often in conflict with the desired performance specification set by the control engineer. For example, it is impossible to add integral action to a feedback control system, typically included to achieve zero steady-state errors, without introducing the negative effect of phase lag. It was the fundamental gain–phase relationship for LTI systems that motivated W.C. Foster and co-workers in 1966 to develop the split-path nonlinear (SPAN) filter, in which they intended to design the gain and phase characteristics separately (Foster, Gieseking, & Waymeyer, 1966). Another fundamental limitation is given by the fact that for a stable closed-loop system, the error step response necessarily overshoots if the open-loop transfer function of the linear plant with LTI controller contains a double integrator, see, e.g., Seron et al. (1997, Theorem 1.3.2). The latter fundamental limitation applies to the majority of motion systems (of which the industrial benchmark study in this paper is an example).

In Aangenent, van de Molengraft, and Steinbuch (2005), Fong and Szeto (1980), Foster et al. (1966) and Zoss, Witte, and Marsch (1968), the SPAN filter was designed as a phase lead filter that does not cause magnitude amplification. It was shown that a controller with such a nonlinear SPAN filter can outperform its linear counterpart with respect to overshoot to a step response. In this paper, we also aim to achieve the same objective, namely, enhancing *transient* performance of linear (motion) systems in terms of overshoot, but we will propose a variant/extension to the SPAN filter, which we will call the split-path nonlinear integrator (SPANI). In contrast to the SPAN filter as in Aangenent et al. (2005), Fong and Szeto (1980), Foster et al. (1966) and Zoss et al. (1968), the SPANI is a *nonlinear integrator* that enforces the integral action to take the same sign as the closed-loop error signal, thereby limiting

☆ This research is financially supported by the Dutch Technology Foundation (STW) under the project "HyperMotion: Hybrid Control for Performance Improvement of Linear Motion Systems" (no. 10953). The material in this paper was partially presented at the 2014 American Control Conference, June 4–6, 2014, Portland, OR, USA.This paper was recommended for publication in revised form by Associate Editor Dragan Nešić under the direction of Editor Andrew R. Teel.

E-mail addresses: s.j.l.m.v.loon@tue.nl (S.J.L.M. van Loon), b.g.b.hunnekens@tue.nl (B.G.B. Hunnekens), m.heemels@tue.nl (W.P.M.H. Heemels), n.v.d.wouw@tue.nl (N. van de Wouw), h.nijmeijer@tue.nl (H. Nijmeijer).

[1] N. van de Wouw is also with the Department of Civil, Environmental and Geo-Engineering, University of Minnesota, Minneapolis, MN 55455 USA, and also with the Delft Center for Systems and Control, Delft University of Technology, Delft, The Netherlands.

http://dx.doi.org/10.1016/j.automatica.2016.01.005
0005-1098/

the amount of overshoot and, as a result, improving the transient performance while still guaranteeing a zero steady-state error in the presence of a constant reference and disturbance signal.

Several other hybrid/nonlinear control strategies for improving the transient performance for linear systems have been proposed in the literature, see Hunnekens (2014) for a recent overview. In this respect, we would like to mention reset control because it exhibits interesting analogies with the SPANI controller proposed in this paper. Firstly, reset control has also been introduced quite some time ago in 1958 (Clegg, 1958), but especially in the last two decades, it has regained attention in both theoretically oriented research, see e.g., Aangenent, Witvoet, Heemels, Van De Molengraft, and Steinbuch (2010), Baños and Barreiro (2012), Beker, Hollot, Chait, and Han (2004), Nešić, Teel, and Zaccarian (2011) and Prieur, Tarbouriech, and Zaccarian (2013), as well as in applications (Baños & Barreiro, 2012; Panni, Waschl, Alberer, & Zaccarian, 2014; Zheng, Chait, Hollot, Steinbuch, & Norg, 2000). Secondly, both strategies have the common feature of using a switching surface (or region) to trigger a change in the control signal, which leads to the injection of discontinuous control signals into an otherwise smooth (and linear) feedback system. Distinctively, reset control employs the same (linear) control law on both sides of the switching surface and a state reset takes place on the switching surface, whereas we will show that due to the construction of the SPANI filter, the dynamics changes after a switch and no state reset takes place. Another important difference is that a reset controller is not capable of achieving a zero-steady state error in the presence of constant reference and disturbance signals, see, e.g., Baños and Barreiro (2012), while the SPANI comes with such guarantees. We will furthermore demonstrate that the proposed (output feedback) controller structure supports the design of all the linear components of the SPANI controlled system using well-known (frequency-domain) loop-shaping techniques. Consequently, the specifically chosen control structure enhances the applicability to industrial control practice since it allows the control engineer to loop-shape the (linear part of the) controller such that it has favorable disturbance attenuation properties, while the SPANI serves as a hybrid *add-on* element that improves the transient performance.

It is well-known that many nonlinear control strategies have in common that closed-loop stability cannot be verified anymore using 'linear' tools such as the Nyquist stability theorem (except in specific cases, see Hunnekens, 2014). Hence, the importance of the development of other testable stability conditions is evident. Despite this fact, none of the works that considered SPAN filters, e.g., Aangenent et al. (2005), Fong and Szeto (1980), Foster et al. (1966) and Zoss et al. (1968), provided such results thus far. In this paper, we propose, therefore, the first testable Lyapunov-based stability conditions for a feedback control system including the newly proposed SPANI controller. This paper extends the preliminary results presented in van Loon, Hunnekens, Heemels, van de Wouw, and Nijmeijer (2014), in particular by presenting the full stability proof and by considering a model-based benchmark study on an industrial pick-and-place machine.

The paper is organized as follows. In Section 2, we introduce and motivate the proposed SPANI filter. Subsequently, in Section 3, we model the resulting closed-loop system as a hybrid system, for which in Section 4 stability conditions are provided. In Section 5, we illustrate the potential of the proposed nonlinear control strategy using a model-based benchmark example of an industrial pick-and-place machine. Finally, we end with conclusions in Section 6.

1.1. Nomenclature

The following notational conventions will be used. Let $\mathbb{R}$ denote the set of real numbers and $\mathbb{R}^n$ the n-fold Cartesian product $\mathbb{R} \times \cdots \times \mathbb{R}$ with the standard Euclidean norm denoted by $\|\cdot\|$. We use $\wedge$, $\vee$ to denote the logical 'and', 'or' operator, respectively. For a matrix $S \in \mathbb{R}^{n\times m}$, we denote by $\mathrm{im} S := \{Sv \mid v \in \mathbb{R}^m\}$ the image of S, and by $\ker S := \{x \in \mathbb{R}^m \mid Sx = 0\}$ its kernel. For two subspaces V, W of $\mathbb{R}^n$, we use $V + W = \{v + w \mid v \in V,\ w \in W\}$ to denote the direct sum, and write $V \oplus W = \mathbb{R}^n$ when $V + W = \mathbb{R}^n$ and $V \cap W = \{0\}$. We call a matrix $P \in \mathbb{R}^{n\times n}$ positive definite and write $P \succ 0$, if P is symmetric (i.e., $P = P^\top$) and $x^\top P x > 0$ for all $x \neq 0$. Similarly, we call $P \prec 0$ negative definite when $-P$ is positive definite. For brevity, we write symmetric matrices of the form $\left[\begin{smallmatrix} A & B \\ B^\top & C \end{smallmatrix}\right]$ as $\left[\begin{smallmatrix} A & B \\ \star & C \end{smallmatrix}\right]$. An $n \times n$ identity matrix is denoted by $I_{n\times n}$, and $O_{k\times l}$ denotes a $k \times l$ matrix with all zero entries. The distance of a vector $x \in \mathbb{R}^n$ to a set $\mathcal{A} \subset \mathbb{R}^n$ is defined by $\|x\|_{\mathcal{A}} := \inf_{y\in\mathcal{A}} \|x - y\|$.

2. Split-path nonlinear integrator

In Section 2.1, we will briefly revisit the original SPAN filter, and, based on these historical developments, propose a new variation/extension to this filter called/being the SPANI filter. Additionally, in Section 2.2, a description of the complete feedback control system will be given.

2.1. Introduction and motivation of the SPANI filter

Originally, the key motivation behind the development of the SPAN filter was to obtain a filter in which the gain and phase could be designed independently (Foster et al., 1966). To achieve such favorable properties, the input signal of the filter, being the closed-loop error e, is divided into two separate branches of which the outputs are multiplied in order to form the control signal u_s, as schematically depicted in Fig. 1. The lower branch contains a sign element, which removes all magnitude information as its output is either ± 1, thereby retaining all *phase* information. The opposite holds for the upper branch as it contains an absolute value element thereby removing all sign information and retaining only the *magnitude* information. Moreover, both branches contain a linear filter $\mathcal{H}_i(s)$, $i \in \{1, 2\}$, $s \in \mathbb{C}$. In Aangenent et al. (2005), Fong and Szeto (1980), Foster et al. (1966) and Zoss et al. (1968), the authors use filters of the form $\mathcal{H}_1(s) = 1/(s + \tau_1)$ (low-pass filter) and $\mathcal{H}_2(s) = (s + \tau_2)/(s + \tau_3)$ (lead filter), with the aim to add phase lead without magnitude amplification.

In this paper, we use the concept of the SPAN filter to propose a new nonlinear controller with the goal to improve the *transient* performance of linear (motion) systems, which is quantified in terms of overshoot to step responses of the closed-loop system, while still guaranteeing a zero steady-state error in the presence of a constant reference and disturbance signal. For that purpose, we select a linear integrator for $\mathcal{H}_1(s)$, i.e., $\mathcal{H}_1(s) = \omega_i/s$, and take $\mathcal{H}_2(s) = 1$. We call this nonlinear filter the *split-path nonlinear integrator* (SPANI), which is schematically represented in the dashed rectangle in Fig. 2, with $\epsilon = 0$. The rationale behind the design of this SPANI filter can be best understood by considering a step response (or the response to a step disturbance) of a system containing integral control. In order to achieve a zero steady-state error, the integrator integrates the error e over time resulting in build-up of the integral buffer. As soon as the error e becomes zero, i.e., $e = 0$, the integrator still has the integrated error stored in its state. Due to the phase lag introduced by the integrator, it takes some time to empty this buffer, causing the error to overshoot. In contrast to a linear integrator, the SPANI enforces the integral action to take the same sign as the error signal, due to the presence of the absolute value and the sign element, see Fig. 2. This results in non-smooth behavior at the time instant when $e = 0$, i.e., an instantaneous switch of the sign of the integral action takes place, thereby inducing a reduction in overshoot.

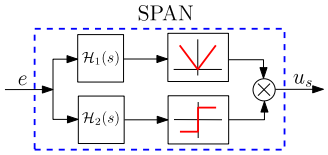

Fig. 1. Schematic representation of the SPAN filter.

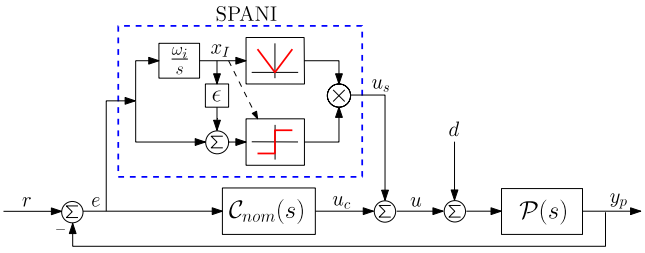

Fig. 2. Feedback loop with plant $\mathcal{P}(s)$, linear controller $\mathcal{C}_{nom}(s)$ and the proposed SPANI controller.

2.2. Description of the control system

The overall feedback configuration used in this paper is shown in Fig. 2. In this figure, $e := r - y_p$ is the tracking error between the reference signal r and the output y_p of the plant with transfer function $\mathcal{P}(s)$, $s \in \mathbb{C}$. Moreover, d denotes an unknown, bounded input disturbance and $u := u_c + u_s$ the total control input, which consists of the control input u_c produced by the linear controller with transfer function $\mathcal{C}_{nom}(s)$ and the control input u_s of the SPANI. The linear part of the closed-loop system consists of a single-input-single-output (SISO) LTI plant

$$\mathcal{P}: \begin{cases} \dot{x}_p &= A_p x_p + B_p u + B_p d \\ y_p &= C_p x_p \end{cases} \tag{1}$$

with state $x_p \in \mathbb{R}^{n_p}$, and a SISO LTI nominal controller

$$\mathcal{C}_{nom}: \begin{cases} \dot{x}_c &= A_c x_c + B_c e \\ u_c &= C_c x_c + D_c e \end{cases} \tag{2}$$

with state $x_c \in \mathbb{R}^{n_c}$. The state (and output) of the integrator $\mathcal{C}_I(s) = \omega_i/s$, with gain $\omega_i \in \mathbb{R}_{>0}$, is defined by $x_I \in \mathbb{R}$. The *sign*-function in the lower branch of the SPANI, see Fig. 2, is formally defined as

$$sign(e, x_I) = \begin{cases} 1 & \text{if } e > 0, \\ 1 & \text{if } e = 0 \text{ and } x_I \geq 0, \\ -1 & \text{if } e = 0 \text{ and } x_I < 0, \\ -1 & \text{if } e < 0, \end{cases} \tag{3}$$

which shows that when $e = 0$, we have $u_s = +x_I$ (the dependence of the sign-function on x_I is denoted by the dashed arrow in Fig. 2). The SPANI controller as in Fig. 2 can be modeled as a switched system with dynamics

$$\text{SPANI}: \begin{cases} \dot{x}_I &= \omega_i e \\ u_s &= \begin{cases} +x_I & \text{if } x_I(\epsilon x_I + e) \geq 0 \\ -x_I & \text{if } x_I(\epsilon x_I + e) < 0, \end{cases} \end{cases} \tag{4}$$

in which $x_I \in \mathbb{R}$ denotes the state of the integrator in the SPANI controller and $\epsilon \in \mathbb{R}_{\geq 0}$. For $\epsilon = 0$, we recover the situation as considered in Section 2.1, i.e., a filter that enforces the integral action to take the *exact* same sign as the error signal. For such a case, the situation where the 'default' integrator is active ($u_s = +x_I$) corresponds to $ex_I \geq 0$ and the situation where the integrator has negative sign ($u_s = -x_I$) corresponds to $ex_I < 0$, see Fig. 3(a) for a representation in the (e, x_I)-plane. The SPANI as in (4) therefore represents a more general class of SPANI controllers,

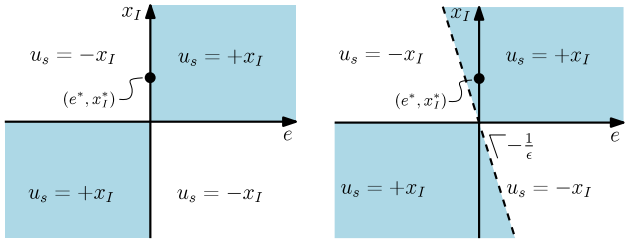

(a) SPANI with $\epsilon = 0$. (b) SPANI with $\epsilon > 0$.

Fig. 3. Schematic representation of the control action of the SPANI in the (e, x_I)-plane.

in which the (typically small) parameter ϵ is associated with tilting of one of the switching boundaries, see Fig. 3(b), and is included to create a SPANI controller with favorable robustness properties compared to the SPANI with $\epsilon = 0$ (which is closer to the classical SPAN filter). The latter claim can be intuitively explained as follows. Consider Fig. 3 and focus first on the SPANI with $\epsilon = 0$, i.e., Fig. 3(a). Note that the desired equilibrium point, with x_I having the equilibrium value x_I^* and e having the equilibrium value $e^* = 0$, i.e., $(e, x_I) = (e^*, x_I^*)$, is located exactly on the switching plane, see Fig. 3(a). Note in this respect that since $e^* = 0$ is enforced by the integral action, it typically requires integral action ($x_I^* \neq 0$) to achieve such zero steady-state error, e.g., if constant disturbances are present. Given the fact that the desired equilibrium is on a switching boundary, small perturbations around this equilibrium may cause the dynamics to switch, resulting in an instantaneous change of sign of u_s. This might result in a large number of consecutive switches, which is highly undesired in many applications. By introducing the tilting parameter ϵ, we ensure that the equilibrium is located strictly inside the set where $x_I(\epsilon x_I + e) \geq 0$, see Fig. 3(b). As a consequence, we ensure that, locally around the equilibrium, no switching occurs. In Section 4, we present conditions that can help in making an appropriate choice for ϵ.

Although the tilting parameter ϵ creates robustness locally around the equilibrium, we cannot provide such guarantees around the switching plane in the remaining part of the state-space. In fact, we will demonstrate in Section 5.2 that in certain situations multiple consecutive switchings can occur. In order to prevent such undesired behavior from happening, a minimal dwell-time argument, see, e.g., Hespanha and Morse (1999) and Solo (1994), is adopted in the switching function of the SPANI as in (4). This will be made more specific and precise in the next section.

3. Hybrid system modeling

In this section, we model the closed-loop system as discussed in Section 2.2, see Fig. 2, in the hybrid system formalism of Goebel, Sanfelice, and Teel (2012), resulting in the description

$$\dot{\chi} = f(\chi, w), \quad \text{if } \chi \in \mathcal{F}, \tag{5a}$$

$$\chi^+ = g(\chi), \quad \text{if } \chi \in \mathcal{J}, \tag{5b}$$

where $\chi \in \mathbb{R}^{n_\chi}$ is the state, $w \in \mathbb{R}^{n_w}$ an exogenous input, $\mathcal{F} \subseteq \mathbb{R}^{n_\chi}$ and $\mathcal{J} \subseteq \mathbb{R}^{n_\chi}$ are the flow set and jump set, respectively, $f: \mathcal{F} \to \mathbb{R}^{n_\chi}$ and $g: \mathcal{J} \to \mathbb{R}^{n_\chi}$ are the flow and jump map, respectively, and χ^+ denotes the value of the state directly after the reset. For the analysis results in this paper, the signals w are typically constant such that the standard notions related to the hybrid framework of Goebel et al. (2012), such as the concept of hybrid time domains and solutions of (5), are applicable. These are reported in the Appendix for convenience of the reader. For more details on this hybrid modeling framework we refer to Goebel et al. (2012).

To obtain a complete closed-loop model of the feedback configuration in Fig. 2, we use the interconnections $e = r - y_p$ and

$u = u_c + u_s$, combine (1), (2) and (4), and define the state-vector $x := [x_p^\top \quad x_c^\top \quad x_I^\top]^\top \in \mathbb{R}^n$, with $n = n_p + n_c + 1$. Moreover, we introduce a timer variable $\tau \in \mathbb{R}_{\geq 0}$ and Boolean $\ell \in \{0, 1\}$, and define the augmented state vector $\chi := [x^\top \quad \tau \quad \ell]^\top \in \Theta$, with $\Theta := \mathbb{R}^{n_x} \times \mathbb{R}_{\geq 0} \times \{0, 1\} \in \mathbb{R}^{n_x+2}$ and $w = [r \quad d]^\top \in \mathbb{R}^2$. Then, the flow map f in (5a) is given by

$$f(\chi, w) = \begin{cases} \left[(\bar{A}_1 x + \bar{B}_r r + \bar{B}_d d)^\top, \quad 1, \quad 0\right]^\top, & \text{when } \ell = 0 \\ \left[(\bar{A}_2 x + \bar{B}_r r + \bar{B}_d d)^\top, \quad 1, \quad 0\right]^\top, & \text{when } \ell = 1 \end{cases} \tag{6a}$$

with

$$\bar{A}_1 := \begin{bmatrix} A_p - B_p D_c C_p & B_p C_c & +B_p \\ -B_c C_p & A_c & 0 \\ -\omega_i C_p & 0 & 0 \end{bmatrix}, \qquad \bar{B}_r := \begin{bmatrix} B_p D_c \\ B_c \\ \omega_i \end{bmatrix}, \tag{6b}$$

$$\bar{A}_2 := \begin{bmatrix} A_p - B_p D_c C_p & B_p C_c & -B_p \\ -B_c C_p & A_c & 0 \\ -\omega_i C_p & 0 & 0 \end{bmatrix}, \qquad \bar{B}_d := \begin{bmatrix} B_p \\ 0 \\ 0 \end{bmatrix}. \tag{6c}$$

We assume that, by proper design, the *linear* controller $\mathcal{C}_{nom}(s) + \mathcal{C}_I(s)$, see Fig. 2, is stabilizing and, as a result, the matrix $\bar{A}_1$ is Hurwitz. However, due to the 'wrong' sign of the integral action, $\bar{A}_2$ will in general not be Hurwitz. In (5), flow according to $\dot{\chi} = f(\chi, w)$, occurs when the state χ is in the flow set given by

$$\mathcal{F} := \big\{\chi \in \Theta \mid \big(\ell = 0 \wedge \big(x_I(\epsilon x_I + e) \geq 0 \\ \vee\, 0 \leq \tau \leq \tau_D\big)\big) \vee \big(\ell = 1 \wedge x_I(\epsilon x_I + e) \leq 0\big)\big\}, \tag{6d}$$

in which $\tau_D \in \mathbb{R}_{\geq 0}$. Note that the state-dependent switching rule of the SPANI controller, see (4), is augmented with a minimal dwell-time argument, see, e.g., Hespanha and Morse (1999) and Solo (1994). To be precise, we only include this time restriction in the first mode (when $\ell = 0$) in which the stable $\bar{A}_1$-dynamics is active and force the system to stay in this mode for at least $\tau_D \in \mathbb{R}_{\geq 0}$ time units. In the second mode (when $\ell = 1$), in which the unstable $\bar{A}_2$-dynamics is active, no time restrictions are imposed.

The jump map g in (5b) is given by

$$g(\chi) := \left[x^\top, \quad 0, \quad 1 - \ell\right]^\top, \tag{6e}$$

and the jump set is given by

$$\mathcal{J} := \big\{\chi \in \Theta \mid \big(\ell = 0 \wedge \big(x_I(\epsilon x_I + e) \leq 0 \wedge \tau \geq \tau_D\big)\big) \\ \vee \big(\ell = 1 \wedge x_I(\epsilon x_I + e) \geq 0\big)\big\}. \tag{6f}$$

Note that $\tau_D > 0$ guarantees that there can be at most two consecutive jumps at one continuous time $t \in \mathbb{R}_{\geq 0}$. In particular, for any solution ϕ to the hybrid system $(\mathcal{F}, f, \mathcal{J}, g)$ and for any $(t, j) \in \operatorname{dom} \phi$, it holds that $(t', j+2) \in \operatorname{dom} \phi$ implies $t' \geq t + \tau_D$.

4. Stability analysis

In this section, we consider constant (step) references $r(t) = r_c$, $t \in \mathbb{R}_{\geq 0}$, and constant disturbances $d(t) = d_c$, $t \in \mathbb{R}_{\geq 0}$, and present LMI-based stability conditions for the hybrid system as in (5), (6). In order to do so, let us define the equilibrium set $\mathcal{A}$ of the hybrid system (5), (6), for which we would like to prove global exponential stability (GES), as follows

$$\mathcal{A} := \{\chi \in \mathcal{F} \cup \mathcal{J} \mid x = x^*\}, \tag{7}$$

in which x^* denotes the equilibrium point satisfying

$$\bar{A}_1 x^* + \bar{B}_r r_c + \bar{B}_d d_c = 0. \tag{8}$$

Note that, x^* (and thus $\mathcal{A}$) depends on the choice of r_c and d_c. Moreover, from (4) it follows that $e^* = 0$ in the equilibrium x^*, such that the equilibrium indeed conforms to the $\bar{A}_1$-dynamics for $\epsilon > 0$, and therefore satisfies (8). Note furthermore that since the system matrix $\bar{A}_1$ is Hurwitz, and thus invertible, (8) has one unique solution x^* for fixed $r_c \in \mathbb{R}$ and $d_c \in \mathbb{R}$.

Theorem 3 below poses sufficient conditions under which GES of the set $\mathcal{A}$ can be guaranteed for the hybrid system (5), (6). Consequently, under these conditions the exact tracking of the constant reference value r_c, and disturbance rejection of the constant disturbance value d_c, are guaranteed. Hereto, let us define what is meant by GES of the set $\mathcal{A}$ in this paper, and introduce some notational conventions used in Theorem 3.

Definition 1. The set $\mathcal{A}$ is said to be GES for the system (5), (6) with $r(t) = r_c$ and $d(t) = d_c$, $t \in \mathbb{R}_{\geq 0}$, if there exist a $\rho \in \mathbb{R}_{>0}$ and $\mu \in \mathbb{R}_{>0}$, such that for all $\chi(0, 0) \in \mathcal{F} \cup \mathcal{J}$, it holds that the corresponding solutions $\chi(t, j)$ to (5), (6) satisfy $\|\chi(t, j)\|_{\mathcal{A}} \leq \rho e^{-\mu t} \|\chi(0, 0)\|_{\mathcal{A}}$ for all $(t, j) \in \operatorname{dom} \chi$.

Remark 2. Note that due to the dwell time condition with $\tau_D > 0$, Definition 1 is in fact equivalent to the definition of GES of $\mathcal{A}$ in Teel, Forni, and Zaccarian (2013). This can be seen by using that for a solution ϕ to (5), (6) it holds that $j \leq 2\frac{t}{\tau_D} + 2$ for any $(t, j) \in \operatorname{dom} \phi$. Nevertheless, we use Definition 1 as we are more interested in the evolution of the state χ over continuous time t.

The matrix $Q \in \mathbb{R}^{(n+2)\times(n+2)}$ is defined by

$$Q := \begin{bmatrix} \bar{A}_2^\top P + P\bar{A}_2 & P\bar{A}_d\bar{A}_1^{-1}\bar{B}_r & P\bar{A}_d\bar{A}_1^{-1}\bar{B}_d \\ \star & 0 & 0 \\ \star & \star & 0 \end{bmatrix} \tag{9}$$

with $\bar{A}_d := \bar{A}_1 - \bar{A}_2$ and a free matrix $P \in \mathbb{R}^{n\times n}$. Furthermore, the matrix $\bar{R} \in \mathbb{R}^{(n+2)\times(n+2)}$ is defined by

$$\bar{R} := \left[\begin{array}{ccc|c|c} 0 & 0 & -\frac{1}{2}C_p^\top & -\frac{1}{2}\gamma_r C_p^\top & -\frac{1}{2}\gamma_d C_p^\top \\ \star & 0 & 0 & 0 & 0 \\ \star & \star & \epsilon & \epsilon\gamma_r & \epsilon\gamma_d \\ \hline \star & \star & \star & \epsilon\gamma_r^2 & \epsilon\gamma_r\gamma_d \\ \hline \star & \star & \star & \star & \epsilon\gamma_d^2 \end{array}\right], \tag{10}$$

for scalars

$$\gamma_r = -\begin{bmatrix} O_{1\times n_p} & O_{1\times n_c} & 1 \end{bmatrix}\bar{A}_1^{-1}\bar{B}_r \tag{11}$$

$$\gamma_d = -\begin{bmatrix} O_{1\times n_p} & O_{1\times n_c} & 1 \end{bmatrix}\bar{A}_1^{-1}\bar{B}_d, \tag{12}$$

related to the integral state in equilibrium

$$x_I^* = \gamma_r r_c + \gamma_d d_c. \tag{13}$$

Finally, let the matrix $M \in \mathbb{R}^{(n+2)\times(n+1)}$ be given by

$$M := \begin{bmatrix} I_{n\times n} & O_{n\times 1} \\ O_{2\times n} & \begin{bmatrix} \gamma_r \\ \gamma_d \end{bmatrix} \end{bmatrix}. \tag{14}$$

Theorem 3. *Consider the hybrid system given by (5), (6), in which $\epsilon > 0$ is fixed and $\tau_D > 0$, and the set $\mathcal{A}$ given by (7). If there exist a positive definite matrix $P \in \mathbb{R}^{n\times n}$ and a constant $\alpha \in \mathbb{R}_{\geq 0}$ satisfying*

$$\bar{A}_1^\top P + P\bar{A}_1 \prec 0 \tag{15}$$

$$M^\top \left(Q - \alpha\bar{R}\right) M \prec 0, \tag{16}$$

then the set $\mathcal{A}$, with $r(t) = r_c$ and $d(t) = d_c$, $t \in \mathbb{R}_{\geq 0}$, is GES for the hybrid system (5), (6).

Proof. We start the proof by introducing the coordinate transformation $\tilde{x} := [\tilde{x}_p^\top \quad \tilde{x}_c^\top \quad \tilde{x}_I^\top]^\top = x - x^*$, and as a result $\|\chi\|_{\mathcal{A}} = \|\tilde{x}\|$.

Next, we will prove that $W(\chi) = V(\tilde{x}) = \tilde{x}^\top P \tilde{x}$, with $P = P^\top \succ 0$, satisfying (15)–(16), is a Lyapunov function for the hybrid system (5), (6). To do so, first observe that

$$c_1\|\tilde{x}\|^2 \leq W(\chi) \leq c_2\|\tilde{x}\|^2, \tag{17}$$

for some $c_2 \geq c_1 > 0$, since $P = P^\top \succ 0$. Second, we are going to show that during flow, we have that, along the solutions of (5), (6),

$$\begin{aligned}\langle \nabla W(\chi), f(\chi)\rangle &\leq -c_3\|\tilde{x}\|^2 \\ &\overset{(17)}{\leq} -c_4 W(\chi) \quad \text{for all } \chi \in \mathcal{F},\end{aligned} \tag{18}$$

for some $c_3 > 0$, $c_4 = \frac{c_3}{c_2} > 0$. To show this, we consider two cases. The first case is given by

$$\chi \in \Theta \quad \text{with } \ell = 0 \wedge \big((x_I(\epsilon x_I + e) \geq 0 \ \vee 0 \leq \tau \leq \tau_D)\big), \tag{19}$$

in which

$$\dot{\tilde{x}} = \bar{A}_1 \tilde{x}. \tag{20}$$

Hence, we obtain that along solutions

$$\dot{V} = \tilde{x}^\top \left(\bar{A}_1^\top P + P\bar{A}_1\right)\tilde{x} \leq -c_5\|\tilde{x}\|^2, \tag{21}$$

for some $c_5 > 0$, due to (15).

The second case is given by

$$\chi \in \Theta \quad \text{with } \ell = 1 \wedge x_I(\epsilon x_I + e) < 0, \tag{22}$$

in which

$$\dot{\tilde{x}} = \bar{A}_2 \tilde{x} - \bar{A}_d x^*, \tag{23}$$

where we used $\bar{A}_d := \bar{A}_1 - \bar{A}_2$, and (8). Note that we can express $x_I(\epsilon x_I + e)$ into the transformed coordinates as follows

$$\psi(\tilde{x}, x^*) := (\tilde{x}_I + x_I^*)(\epsilon\tilde{x}_I + \epsilon x_I^* - C_p\tilde{x}_p), \tag{24}$$

using $e = r_c - C_p x_p = r_c - C_p(\tilde{x}_p + x_p^*) = -C_p\tilde{x}_p$, since $r_c - C_p x_p^* = e^* = 0$. Let us introduce the augmented vector $\tilde{x}_a := [\tilde{x}^\top \quad r_c \quad d_c]^\top$, and use (11), (12) to express x_I^* in terms of r_c and d_c, as in (13). This allows us to write the switching function $\psi(\tilde{x}, x^*)$ in (24) in a quadratic form $\psi(\tilde{x}_a) = \tilde{x}_a^\top \bar{R}\tilde{x}_a$ (with some slight abuse of notation), where $\bar{R}$ is as defined in (10). Now we obtain

$$\begin{aligned}\dot{V} &= \tilde{x}^\top \left(\bar{A}_2^\top P + P\bar{A}_2\right)\tilde{x} - x^{*\top}\bar{A}_d^\top P\tilde{x} - \tilde{x}^\top P\bar{A}_d x^*, \\ &= \tilde{x}_a^\top Q\tilde{x}_a,\end{aligned} \tag{25}$$

for Q as defined in (9). Hence, we need to show that there exists a $c_6 > 0$ such that

$$\tilde{x}_a^\top Q\tilde{x}_a \leq -c_6\|\tilde{x}\|^2, \quad \text{when } \ell = 1 \wedge \psi(\tilde{x}_a) < 0. \tag{26}$$

To prove this, observe that, for M defined in (14) and $\mathrm{im}H \subseteq \ker Q$ with H defined as

$$H := \begin{bmatrix} O_{1\times n} & -\gamma_d & \gamma_r \end{bmatrix}^\top, \tag{27}$$

in which $\gamma_d \neq 0$ and $\gamma_r \neq 0$, it holds that $\mathrm{im}M \oplus \mathrm{im}H = \mathbb{R}^n$. Hence, we can write $\tilde{x}_a = M\tilde{m} + h$ for some $\tilde{m} \in \mathbb{R}^{(n+1)\times 1}$ and $h \in \mathrm{im}H$. These facts lead to

$$\begin{aligned}\tilde{x}_a^\top Q\tilde{x}_a &= (M\tilde{m} + h)^\top Q(M\tilde{m} + h) \\ &= \tilde{m}^\top M^\top QM\tilde{m}\end{aligned} \tag{28}$$

in which we used $\mathrm{im}H \subseteq \ker Q$ (and thus $Qh = 0$). In addition, note that, $\tilde{x}_a^\top \bar{R}\tilde{x}_a < 0$ implies that $\tilde{m}^\top M^\top \bar{R}M\tilde{m} < 0$, because $\mathrm{im}H \subseteq \ker \bar{R}$ (and thus $\bar{R}h = 0$). Hence, for the case where $\ell = 1$ and $\tilde{x}_a^\top \bar{R}\tilde{x}_a < 0$ we obtain

$$\begin{aligned}\tilde{m}^\top M^\top QM\tilde{m} &\leq \tilde{m}^\top M^\top (Q - \alpha\bar{R})M\tilde{m} \\ &\overset{(16)}{\leq} -c_7\|\tilde{m}\|^2,\end{aligned} \tag{29}$$

for some $c_7 > 0$, $\alpha \geq 0$. Using now that $\|\tilde{m}\| \geq c_8\|M\tilde{m}\|$ for some $c_8 > 0$, due to M having full column rank, and $\|M\tilde{m}\| \geq \|\tilde{x}\|$, in view of the form of M, we obtain (26) for $c_6 = c_7c_8 > 0$, as desired. This establishes (18) in which $c_3 = \min\{c_5, c_6\}$.

As a last step, we study the behavior during jumps, which leads to

$$W(g(\chi)) - W(\chi) = 0 \quad \text{for all } \chi \in \mathcal{J}, \tag{30}$$

due to (6e). This, together with the fact that $\tau_D > 0$ guarantees that there can be at most two consecutive jumps, and thus the hybrid time domain of solutions ϕ to (5), (6) is unbounded in the t-direction, i.e., $\sup\{t \mid (t, j) \in \mathrm{dom}\,\phi\} = \infty$. This implies that along a solution χ of the hybrid system (5), (6), the inequality in (18) and (30) combined implies

$$W(\chi(t, j)) \leq e^{-c_4 t} W(\chi(0, 0)), \tag{31}$$

for all $(t, j) \in \mathrm{dom}\,\chi$ and all $t \in \mathbb{R}_{\geq 0}$. Hence, GES, in the sense of Definition 1, of the set $\mathcal{A}$ of the hybrid system (5), (6) for $r(t) = r_c$ and $d(t) = d_c$, $t \in \mathbb{R}_{\geq 0}$, is obtained with $\rho = \sqrt{\frac{c_2}{c_1}}$ and $\mu = \frac{1}{2}c_4$. This completes the proof. □

Remark 4. Theorem 3 guarantees that solutions of the closed-loop system converge exponentially (as a function of continuous time t) to the set on which $e = 0$ for all $\tau_D > 0$ and $r(t) = r_c$, $d(t) = d_c$, $t \in \mathbb{R}_{\geq 0}$. In addition, for $\tau_D = 0$ the closed-loop dynamics can be represented by a continuous-time switched linear system given by

$$\dot{x} = \begin{cases} \bar{A}_1 x + \bar{B}_r r + \bar{B}_d d & \text{if } x_I(\epsilon x_I + e) \geq 0 \quad \text{(a)} \\ \bar{A}_2 x + \bar{B}_r r + \bar{B}_d d & \text{if } x_I(\epsilon x_I + e) < 0, \quad \text{(b)} \end{cases} \tag{32}$$

with output $y_p = C_p x_p$. In such switched systems, sliding modes can occur when the vector fields on both sides of the switching surface point towards each other, see, e.g., Filippov (1988). However, it can be shown that, based on a Lyapunov analysis of the convex combination between the dynamics on both sides of the switching plane, the occurrence of sliding modes (if they exist) does not change the GES of $\mathcal{A}$ under the hypothesis of Theorem 3. For details, see Hunnekens (2014).

5. Case study on a pick-and-place machine

In this section, we consider a simulation study based on an industrial pick-and-place machine used to place electrical components, such as resistors, capacitors, integrated circuits etc., with a high speed and high precision on a printed circuit board (PCB) (Assembléon, 2015). The working principle of a pick-and-place machine is as follows: The first step is to place the PCB within the working area of the placement head, in the second step the placement head picks up an electrical component, and in the third step the placement head is navigated to a pre-described position on the PCB where it should place the component. Finally, in the fourth step, the component is placed on the PCB as soon as all positioning tolerances are met. In this case study, we focus particularly on the third step with the goal to enable the fourth step to start as soon as possible. Namely, the placement of the electrical component on the PCB in the fourth step can only be finalized when the closed-loop error e, related to step three, has converged within a pre-described error bound. Therefore, our objective is to study if we can increase the machine throughput by achieving a faster convergence of the closed-loop error to its specified error bound by replacing the linear integrator $\mathcal{C}_I(s)$ by a SPANI of the form (4) (with the same integrator gain ω_I).

5.1. Simulation model

A schematic representation of the simulation model is depicted in Fig. 4. In this figure, the plant $\mathcal{P}(s)$ is identified based on measured frequency response data, resulting in a 4th-order model. The plant will be controlled by a proportional–integral–derivative

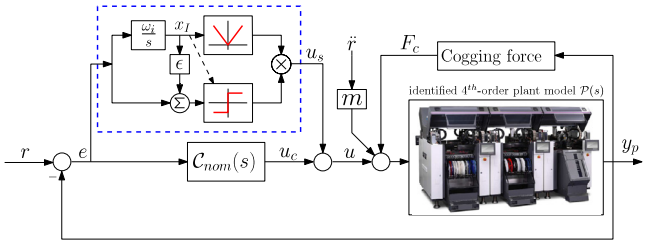

Fig. 4. Schematic representation of the simulation model.

(PID)-type controller $\mathcal{C}_{nom}(s) + \mathcal{C}_I(s)$, in which $\mathcal{C}_{nom}(s)$ consists of a PD-controller and a 2nd-order low-pass filter. Additionally, as in many industrial motion controllers, acceleration feedforward is used, with gain m that represents the estimated plant mass, to compensate for the low-frequency rigid-body plant dynamics. Cogging forces, which are position-dependent force disturbances caused by the magnetic interaction between the permanent magnets and the motor coils, are known to be the main disturbance source in this particular application. Based on identification experiments, we modeled this cogging disturbance force as a sinusoidal position-dependent force given by

$$F_c(y_p) = A_{F_c} \sin\left(\tfrac{\delta_p}{2\pi} y_p + \phi_{F_c}\right), \tag{33}$$

in which A_{F_c} denotes the maximum cogging force, δ_p the pitch between the magnets and ϕ_{F_c} a phase shift tuned on the basis of measurement data.

Remark 5. Although there exist feedforward techniques that can compensate for such (repetitive) cogging force disturbances, for instance using iterative learning control, see e.g., Janssens, Pipeleers, and Swevers (2013) and van Berkel, Rotariu, and Steinbuch (2007), or look-up tables, these disturbances vary from machine to machine and often manufacturers do not have the resources to implement such techniques on each machine separately. Moreover, the vast majority of industrial applications will be subject to disturbances that cannot be easily identified, and thus perfectly compensated for by feedforward control. Hence, integral action in the controller is still necessary in order to achieve zero steady-state errors.

In the following sections, we compare the transient performance of a linear controller with a controller in which the linear integrator is replaced by a SPANI. In Section 5.2, we consider the situation in which no dwell-time is included, i.e., $\tau_D = 0$. We show that the transient performance will increase by using a SPANI, but also that $\tau_D = 0$ might yield some undesired behavior in certain situations. In Section 5.3, we demonstrate that this undesired behavior can be prevented by including dwell-time restrictions as already introduced in Section 3.

5.2. Transient performance comparison with $\tau_D = 0$

In this section, we take $\tau_D = 0$ and study the response for two 4th-order reference trajectories corresponding to two different positions on the PCB where the electrical component should be placed, i.e., the first reference trajectory has an end position of 200 mm and the second of 105 mm. Note that due to the position-dependent cogging forces, this results in two different disturbance situations that the SPANI controller will have to cope with.

Let us first consider the reference with an end position of 200 mm. Fig. 5 shows the error[2] profiles using; a linear controller

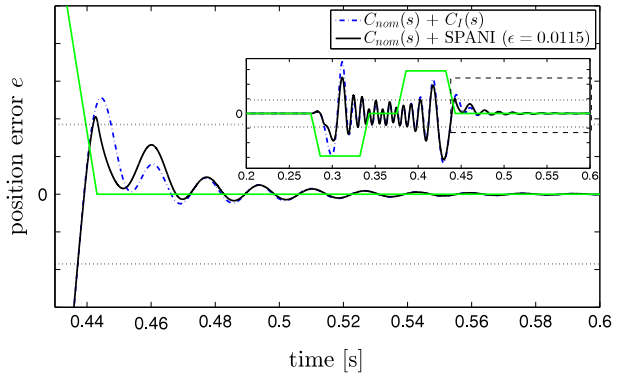

Fig. 5. Error profile for the region of interest using a 4th-order reference trajectory with an end position of 200 mm. For the sake of clarity, a scaled acceleration profile is shown in green and a smaller figure is added showing the entire time span in which the region of interest is indicated by the dashed rectangle. (For interpretation of the references to color in this figure legend, the reader is referred to the web version of this article.)

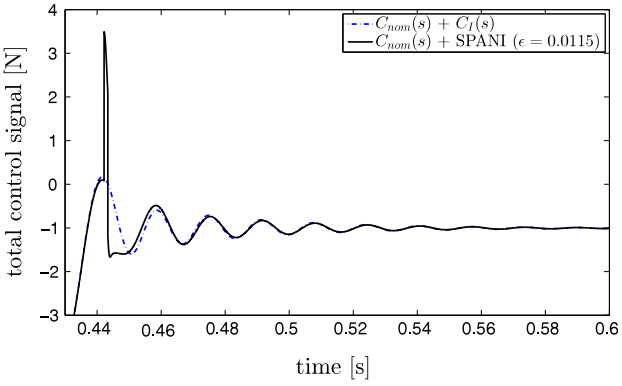

Fig. 6. Total control signal for the linear controller $\mathcal{C}_{nom} + \mathcal{C}_I$, and for $\mathcal{C}_{nom}$ + SPANI.

(dash-dotted blue), and in solid black the error profile obtained if we replace the linear integrator $\mathcal{C}_I$ by a SPANI of the form (4) (with the same gain ω_I) and $\epsilon = 0.0115$. This value for ϵ is motivated by the conditions of Theorem 3 and Remark 4. In fact, by verifying these conditions we can guarantee that the equilibrium x^* of (32) is GES for all $\epsilon \geq 0.0115$. As indicated in Fig. 5, compared to the linear case, an improved, and asymptotically stable, response can be obtained using a SPANI. Note that with 'improved', we mean both a reduction in overshoot and a faster convergence to the error bound (depicted by the horizontal dotted lines). This is in correspondence with the two performance objectives previously defined in Section 5.1. Firstly, we observe a significant overshoot reduction of ∼20% almost immediately after the pick-and-place robot reaches its end-position (∼0.443 s in Fig. 5), while an even more significant overshoot reduction is achieved in the response around $t = 0.3$ s, see the smaller figure inside Fig. 5. Secondly, almost immediately after the pick-and-place robot reaches its end-position (∼0.443 s in Fig. 5) the error signal of the system with SPANI has converged within the error bound, thereby again outperforming the linear controller. These performance improvements are achieved by only two switches (in the region of interest) of the SPANI filter, see Fig. 6 in which the total control signal $u = u_c + u_s$ is depicted.

Let us now consider the reference profile with an end position of 105 mm. The error profiles of the linear controller and the nominal controller with SPANI and $\epsilon = 0.0115$ are depicted in Fig. 7(a), which again indicates that the SPANI controller outperforms the linear controller with respect to overshoot (by ∼43% in this case)

[2] To protect the interests of the manufacturer, all figures in this section have either been scaled or use blank axes in terms of units.

and convergence within the error bound. However, it also reveals the following undesired behavior:

- For $t \in [0.43, 0.48]$: The error shows fast oscillatory behavior, resulting from a large number of switches;
- For $t \in [0.48, 0.52]$: An unexpected 'peak' in the error signal occurs while we expect to converge smoothly towards $e = 0$.

Both these phenomena are undesired and can be explained by considering Fig. 7(b)–(c), in which we consider the (e, x_I)-plot Fig. 7(b), and the integral action x_I and the output u_s of the SPANI versus time in Fig. 7(c). In these figures, the equilibrium point is depicted by point C, which, for this particular disturbance situation, requires positive integral action ($\sim x_I^* = 0.286$) to compensate for the cogging disturbance force at the setpoint. However, as indicated in Fig. 7(b)–(c), the integral action x_I has the wrong sign (up till point B). Still, up to point A in Fig. 7(b)–(c), the SPANI output u_s delivers, by means of many switches in the control signal u_s, *on average* enough integral action to approximately compensate for the cogging disturbance. However, after point A in the figure, $|x_I|$ is too small such that the SPANI cannot compensate for the cogging disturbance anymore. This results in a build-up of error, causing the peak in the error signal as depicted in Fig. 7(a) and Fig. 7(b)–(c). Eventually, after point B in Fig. 7, the integral state x_I becomes positive and converges to the equilibrium in point C.

5.3. Transient performance comparison with $\tau_D > 0$

In this section, we show that adding a minimal dwell-time condition $\tau_D > 0$, as discussed in Section 3, can alleviate this undesired behavior. Including dwell-time logic in the switching condition of the SPANI filter requires the tuning of the new parameter τ_D, which according to Theorem 3 cannot cause instability of the set $\mathcal{A}$. Simulation results for such a SPANI filter with dwell-time restriction are depicted in Fig. 8 using $\tau_D = 0.0063$ s. The working principle of the new switching rule can be explained best by considering Fig. 8(b), in which the (e, x_I)-plane is shown. In point D, the response of the SPANI-controlled system reaches the switching plane for the first time and switches from mode 1 (red) to mode 2 (green) following the $\bar{A}_2$-dynamics. We stay in this mode until we reach the switching plane again at point E, where we switch back to mode 1. Apparently, the vector field of the $\bar{A}_1$-dynamics directs towards the switching plane but at the moment of crossing (point F) the dwell-time condition $\tau \geq \tau_D$ is not yet satisfied. Hence, no switch takes place and it takes until point G at which the dwell-time condition is satisfied. At that moment in time, we do not satisfy the condition $x_I(\epsilon x_I + e) \geq 0$, resulting in a switch to mode 2.

Let us now compare this result to the previous situation, i.e., as depicted in Fig. 7. Concentrating first on Figs. 7(b) and 8(b), we observe that up to point F the error profiles are identical.[3] As a result, the first peak in the error profiles (around ∼0.42 s) of Figs. 7(a) and 8(a) is identical. However, for sufficiently large τ_D, this does not apply to the second peak (around ∼0.43 s) in the error profile. This can be explained by considering point F; for the case $\tau_D = 0$ a switch to mode 2 takes place at point F causing an immediate change in the vector field. However, for the case with $\tau_D = 0.0063$, no switch takes place up till point G, thereby causing the system to reside longer in mode 1, which, in turn, causes the error to overshoot more in this particular situation. Therefore, including such dwell-time logic into the switching condition might result in a (slight) decrease of potential transient performance benefits. Nevertheless, it is clear from Fig. 8 that the dwell-time condition prevents the undesirably large number of switches in the control signal as in Fig. 7(c) for the case $\tau_D = 0$. Not only the number of switches has decreased, see Fig. 8(c), the error profile also now gradually converges to $e = 0$ without the occurrence of a sudden unwanted peak (compare Figs. 7(a) and 8(a)).

[3] This applies in general for sufficiently small τ_D such that at point D in Fig. 8(b), we satisfy the dwell-time condition $\tau \geq \tau_D$.

5.4. Final note

The main motivation for and the rationale behind the design of the SPANI is to improve the transient performance of linear systems by reducing overshoot, which is successfully demonstrated in this section. It is important to note that, in general, it is hard to give any guarantees on the settling behavior. In the benchmark study presented in this section, we satisfied both our objectives, i.e., reducing overshoot and a faster convergence to an error bound. The secondary objective cannot always be guaranteed and it depends on the tuning of the dwell-time parameter τ_D and the disturbance situation at hand. However, the primary objective of reducing overshoot is satisfied in all (considered) cases.

Remark 6. The interesting reader may consult (Hunnekens, 2014) for additional discussions and comments.

6. Conclusions

In this paper, we proposed the split-path nonlinear integrator (SPANI) as a novel variation/extension to a nonlinear filter that was originally introduced in the late 1960s. The SPANI is especially designed for transient performance improvement of linear systems. In particular, we focussed on the transient performance improvement in terms of overshoot to step responses, while being able to achieve zero steady-state errors in the presence of constant disturbances. By means of simulations it was demonstrated that, in particular situations, the SPANI controller can indeed outperform its linear counterpart. Moreover, a formal stability analysis was presented for this novel feedback control configuration with SPANI based on a hybrid dynamical system model for the closed-loop dynamics. Based on this hybrid modeling formalism, sufficient Lyapunov-based stability conditions have been provided in terms of linear matrix inequalities. These conditions proved to be useful in the design of the SPANI. A nice additional feature of the SPANI is that it is easy to apply in industrial practice as all the individual components of the proposed nonlinear controller can be synthesized using classical loop-shaping techniques. By presenting a fundamental modeling framework based on hybrid models and corresponding stability analysis tools, and also showing both the advantages and disadvantages of the SPANI controller, a complete design framework for SPANI controllers has been laid down.

Appendix. Hybrid systems notation

According to Goebel et al. (2012), a set $E \subset \mathbb{R}_{\geq 0} \times \mathbb{N}$ is a compact hybrid time domain if $E = \cup_{j=0}^{J-1}([t_j, t_{j+1}], j)$ for some finite sequence of times $0 = t_0 \leq t_1 \leq t_2, \ldots \leq t_J$. It is a hybrid time domain if for all $(T, J) \in E$, $E \cap ([0, T] \times \{0, 1, \ldots, J\})$ is a compact hybrid time domain. A function $\phi : E \to \mathbb{R}^n$ is a hybrid arc if E is a hybrid time domain and if for each $j \in \mathbb{N}$, the function $t \to \phi(t, j)$ is locally absolutely continuous on the interval $I^j = \{t : (t, j) \in E\}$. A hybrid arc ϕ is a solution to the hybrid system $(\mathcal{F}, f, \mathcal{J}, g)$ if $\phi(0, 0) \in \bar{\mathcal{F}} \cup \mathcal{J}$, and

(1) for all $j \in \mathbb{N}$ such that $I^j = \{t : (t, j) \in \operatorname{dom}\phi\}$ has nonempty interior

$$\phi(t, j) \in \mathcal{F} \qquad \text{for all } t \in \operatorname{int} I^j$$
$$\dot{\phi}(t, j) \in f(\phi(t, j), w(t)) \quad \text{for almost all } t \in I^j$$

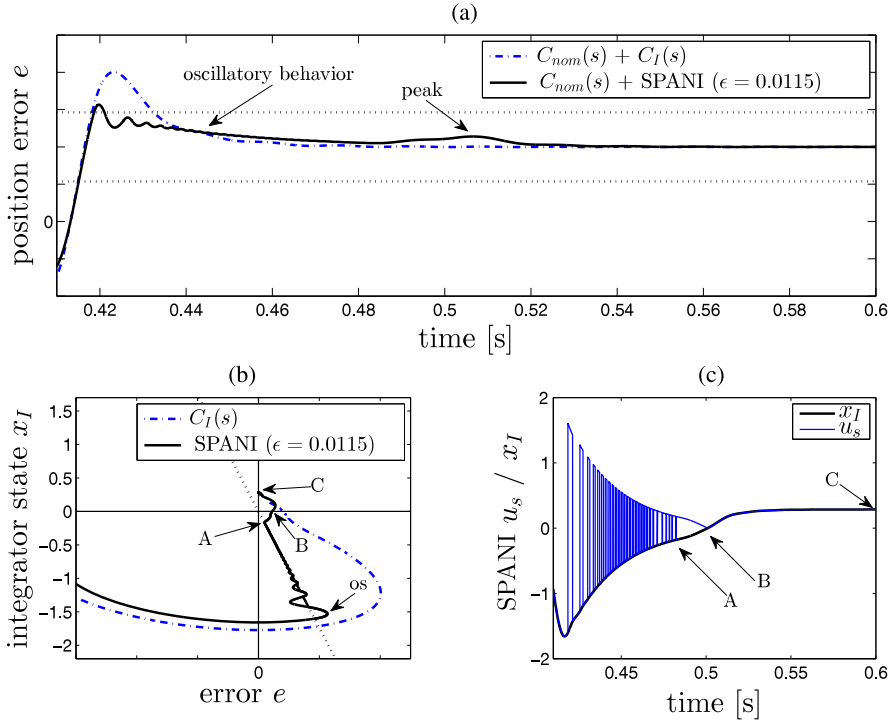

Fig. 7. (a) Error profile for the region of interest using a 4th-order reference trajectory with an end position of 105 mm. (b) Error e versus integral action x_I. (c) Time versus output u_s of the SPANI and integral action x_I.

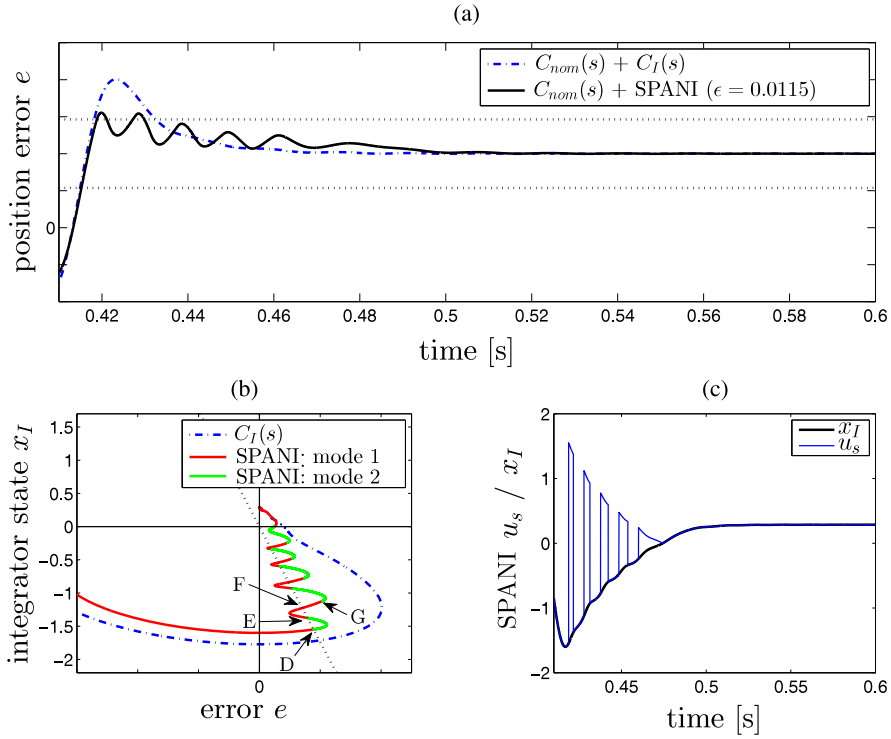

Fig. 8. (a) Error profile for the region of interest using a 4th-order reference trajectory with an end position of 105 mm. (b) Error e versus integral action x_I. (c) Time versus output u_s of the SPANI and integral action x_I. (For interpretation of the references to color in this figure legend, the reader is referred to the web version of this article.)

(2) for all $(t, j) \in \operatorname{dom} \phi$ such that $(t, j+1) \in \operatorname{dom} \phi$,

$$\phi(t, j) \in \mathcal{J},$$
$$\phi(t, j+1) \in g(\phi(t, j)).$$

References

Aangenent, W.H.T.M., van de Molengraft, M.J.G., & Steinbuch, M. (2005). Nonlinear control of a linear motion system. In *IFAC World Congress, vol. 16*.

Aangenent, W. H. T. M., Witvoet, G., Heemels, W. P. M. H., Van De Molengraft, M. J. G., & Steinbuch, M. (2010). Performance analysis of reset control systems. *International Journal of Robust and Nonlinear Control, 20*(11), 1213–1233.

Assembléon (2015). http://www.assembleon.com/.

Baños, A., & Barreiro, A. (2012). *Reset control systems*. Springer.

Beker, O., Hollot, C. V., Chait, Y., & Han, H. (2004). Fundamental properties of reset control systems. *Automatica, 40*(6), 905–915.

Clegg, J. (1958). A nonlinear integrator for servomechanisms. *Transactions of the American Institute of Electrical Engineers, 77*(Part-II), 41–42.

Filippov, A. F. (1988). *Differential equations with discontinuous righthand sides*. Dordrecht, The Netherlands: Kluwer.
Fong, M. H., & Szeto, W. W. (1980). Application of a nonlinear filter to a conditionally stable system. *International Journal of Control*, *32*(6), 963–981.
Foster, W. C., Gieseking, D. L., & Waymeyer, W. K. (1966). A nonlinear filter for independent gain and phase (with application). *Transactions of the ASME Journal of Basic Engineering*, *78*, 457–462.
Freudenberg, J., Middleton, R., & Stefanpoulou, A. (2000). A survey of inherent design limitations. In *Proc. American control conf., Vol. 5* (pp. 2987–3001).
Goebel, R., Sanfelice, R. G., & Teel, A. R. (2012). *Hybrid dynamical systems: modeling, stability and robustness*. Princeton University Press.
Hespanha, J.P., & Morse, A.S. (1999). Stability of switched systems with average dwell-time. In *Proc. 38th IEEE conf. decision and control, Vol. 3* (pp. 2655–2660).
Hunnekens, B. G. B. (2014). *Performance optimization of hybrid controllers for linear motion systems*. (Ph.D. thesis), Eindhoven University of Technology.
Janssens, P., Pipeleers, G., & Swevers, J. (2013). A data-driven constrained norm-optimal iterative learning control framework for LTI systems. *IEEE Transactions on Control Systems Technology*, *21*(2), 546–551.
Nešić, D., Teel, A. R., & Zaccarian, L. (2011). Stability and performance of siso control systems with first-order reset elements. *IEEE Transactions on Automatic Control*, *56*(11), 2567–2582.
Panni, F. S., Waschl, H., Alberer, D., & Zaccarian, L. (2014). Position regulation of an EGR valve using reset control with adaptive feedforward. *IEEE Transactions on Control Systems Technology*, *22*(6), 2424–2431.
Prieur, C., Tarbouriech, S., & Zaccarian, L. (2013). Lyapunov-based hybrid loops for stability and performance of continuous-time control systems. *Automatica*, *49*(2), 577–584.
Seron, M. M., Braslavsky, J. H., & Goodwin, G. C. (1997). *Fundamental limitations in filtering and control*. Berlin: Springer.
Solo, V. (1994). On the stability of slowly time-varying linear systems. *Mathematics of Control, Signals, and Systems*, *7*(4), 331–350.
Teel, A. R., Forni, F., & Zaccarian, L. (2013). Lyapunov-based sufficient conditions for exponential stability in hybrid systems. *IEEE Transactions on Automatic Control*, *58*(6), 1591–1596.
van Berkel, K., Rotariu, I., & Steinbuch, M. (2007). Cogging compensating piecewise iterative learning control with application to a motion system. In *Proc. American control conf.* (pp. 1275–1280).
van Loon, S.J.L.M., Hunnekens, B.G.B., Heemels, W.P.M.H., van de Wouw, N., & Nijmeijer, H. (2014). Transient performance improvement of linear systems using a split-path nonlinear integrator. In *Proc. American control conf.* (pp. 341–346).
Zheng, Y., Chait, Y., Hollot, C. V., Steinbuch, M., & Norg, M. (2000). Experimental demonstration of reset control design. *Control Engineering Practice*, *8*(2), 113–120.
Zoss, L.M., Witte, A.G., & Marsch, J.E. (1968). A nonlinear three response controller with two response adjustment. In *Proc. of the Advances in intrumentation* (pp. 1–6).

S.J.L.M. (Bas) van Loon received the M.Sc. degree in Mechanical Engineering from Eindhoven University of Technology (TU/e), Eindhoven, the Netherlands, in 2011. He is currently pursuing the Ph.D. degree at the Department of Mechanical Engineering, TU/e. His current research interests include modeling, analysis and control of hybrid systems and nonlinear control of linear systems.

Bram Hunnekens (born 1987) received the M.Sc. degree (cum laude) in Dynamics and Control from Eindhoven University of Technology, Eindhoven, the Netherlands, in 2011. In 2015, he received the Ph.D. degree at the Department of Mechanical Engineering, Eindhoven University. Since 2015, he is affiliated with Demcon Advanced Mechatronics, Eindhoven, The Netherlands. His research interests include nonlinear control of linear motion systems and performance-optimal nonlinear controller synthesis.

W.P.M.H. Heemels received the M.Sc. degree in Mathematics and the Ph.D. degree in Control Theory (both summa cum laude) from the Eindhoven University of Technology (TU/e), Eindhoven, the Netherlands, in 1995 and 1999, respectively. From 2000 to 2004, he was with the Electrical Engineering Department, TU/e, as an Assistant Professor and from 2004 to 2006 with the Embedded Systems Institute (ESI) as a Research Fellow. Since 2006, he has been with the Department of Mechanical Engineering, TU/e, where he is currently a Full Professor in the Control Systems Technology Group. He held visiting research positions at the Swiss Federal Institute of Technology (ETH), Zurich, Switzerland (2001) and at the University of California at Santa Barbara (2008). In 2004, he was also at the Research and Development Laboratory, Océ, Venlo, the Netherlands. His current research interests include hybrid and cyber–physical systems, networked and event-triggered control systems and constrained systems including model predictive control. He served/s on the editorial boards of Automatica, Nonlinear Analysis: Hybrid Systems, Annual Reviews in Control, and IEEE Transactions on Automatic Control. He was a recipient of a personal VICI grant awarded by NWO (The Netherlands Organisation for Scientific Research) and STW (Dutch Technology Foundation) and is a fellow of the IEEE.

Nathan van de Wouw (born, 1970) obtained his M.Sc.-degree (with honours) and Ph.D.-degree in Mechanical Engineering from the Eindhoven University of Technology, Eindhoven, the Netherlands, in 1994 and 1999, respectively. He currently holds a full professor position at the Mechanical Engineering Department of the Eindhoven University of Technology, the Netherlands. He also holds an adjunct full professor position at the University of Minnesota, USA and a (part-time) full professor position at the Delft University of Technology, the Netherlands. In 2000, He has been working at Philips Applied Technologies, Eindhoven, The Netherlands, and, in 2001, he has been working at the Netherlands Organisation for Applied Scientific Research (TNO), Delft, The Netherlands. He has held positions as a visiting professor at the University of California Santa Barbara, USA, in 2006/2007, at the University of Melbourne, Australia, in 2009/2010 and at the University of Minnesota, USA, in 2012 and 2013. He has published a large number of journal and conference papers and the books 'Uniform Output Regulation of Nonlinear Systems: A convergent Dynamics Approach' with A.V. Pavlov and H. Nijmeijer (Birkhauser, 2005) and 'Stability and Convergence of Mechanical Systems with Unilateral Constraints' with R.I. Leine (Springer-Verlag, 2008). He currently is an Associate Editor for the journals "Automatica" and "IEEE Transactions on Control Systems Technology". In 2015, he received the IEEE Control Systems Technology Award "For the development and application of variable-gain control techniques for high-performance motion systems". His current research interests are the analysis and control of nonlinear/hybrid systems, with applications to vehicular platooning, high-tech systems, resource exploration, smart energy systems and networked control systems.

Henk Nijmeijer (1955) obtained his M.Sc.-degree and Ph.D.-degree in Mathematics from the University of Groningen, Groningen, the Netherlands, in 1979 and 1983, respectively. From 1983 till 2000 he was affiliated with the Department of Applied Mathematics of the University of Twente, Enschede, the Netherlands. Since, 1997 he was also part-time affiliated with the Department of Mechanical Engineering of the Eindhoven University of Technology, Eindhoven, the Netherlands. Since 2000, he is a full professor at Eindhoven, and chairs the Dynamics and Control group. He has published a large number of journal and conference papers, and several books, he was editor in chief of the Journal of Applied Mathematics until 2009, corresponding editor of the SIAM Journal on Control and Optimization, and board member of the International Journal of Control, Automatica, Journal of Dynamical Control Systems, International Journal of Bifurcation and Chaos, International Journal of Robust and Nonlinear Control, Journal of Nonlinear Dynamics and the Journal of Applied Mathematics and Computer Science, and Hybrid Systems. He is editor of Communications in Nonlinear Science and Numerical Simulations. He is a fellow of the IEEE since 2000 and was awarded in 1990 the IEE Heaviside premium. He is honorary knight of the 'golden feedback loop' (NTNU), since 2011. His research interests are in the broad scope of dynamics and control and their applications. He is since 2011 an IFAC Council Member and as of January 2015 Scientific Director of the graduate school DISC (Dutch Institute of Systems and Control).